J|A|C|S
COMMUNICATIONS

Published on Web 11/01/2008

Phosphate Diester and DNA Hydrolysis by a Multivalent, Nanoparticle-Based Catalyst

Renato Bonomi,[†] Francesco Selvestrel,[†] Valentina Lombardo,[‡] Claudia Sissi,[‡] Stefano Polizzi,[§] Fabrizio Mancin,*[,†] Umberto Tonellato,[†] and Paolo Scrimin*[,†]

Dipartimento di Scienze Chimiche and CNR-ITM, Università di Padova, Padova, Italy, Dipartimento di Scienze Farmaceutiche, Università di Padova, Padova, Italy, and Dipartimento di Chimica Fisica, Università di Venezia, Venice, Italy

Received March 11, 2008; E-mail: fabrizio.mancin@unipd.it; paolo.scrimin@unipd.it

DNA phosphodiester bonds are hardly hydrolyzed under neutral conditions and represent a real challenge for chemists but not for enzymes, which succeed in this task exploiting a perfect organization of metal ions and organic groups in their active sites.[1] Synthetic catalysts for DNA hydrolysis with good activity have been obtained by using Ce(IV), Cu(II), and Fe(III) complexes, but Zn(II)-based agents are generally less efficient.[1] Zn(II) is the metal ion preferred by hydrolytic enzymes, and it is nontoxic, redox inactive, and bioavailable. Hence, efficient Zn(II)-based catalysts would constitute a remarkable achievement particularly for biomedical applications.[1a,b] It is common wisdom that good catalysts for phosphate cleavage require properly designed multinuclear catalytic sites. We describe here a new catalyst obtained by self-assembling multiple copies of the thiolated ligand **1** (Chart 1) on the surface of monolayer-protected gold nanoparticles (MPGNs).[2] High activity and a new mode of action arise from the multivalent nature of the catalyst.[3]

Zn(II) complexes of BAPA (Chart 1) derivatives efficiently elicit the cooperation between metal Lewis acid activation and hydrogen bonding to achieve increased hydrolytic activity toward phosphate diesters.[4,5] For this reason, thiol **1** was selected as a Zn(II)-ligand for the preparation of the hydrolytic MPGNs. Thiol **2**, bearing a tri(ethyleneglycol) unit, was also introduced in the coating monolayers to improve water solubility of the nanoparticles. MPGNs (1.8 ± 0.7 nm gold core diameters) were prepared following our recently reported two-step protocol.[2d] Two different **1** to **2** ratios were realized in the coating monolayer (1:9 and 4:6) corresponding to the average formulas $Au_{201}\mathbf{1}_7\mathbf{2}_{64}$ ($\mathbf{1}_{0.1}$-MPGN) and $Au_{201}\mathbf{1}_{28}\mathbf{2}_{43}$ ($\mathbf{1}_{0.4}$-MPGN), respectively (see Supporting Information, SI).

Incubation of **1**-MPGN-Zn(II) with the DNA model substrate bis-*p*-nitrophenyl phosphate (BNP) in 93:7 water/methanol buffered solutions at 40 °C resulted in substrate cleavage with the concomitant formation of *p*-nitrophenolate and *p*-nitrophenyl phosphate (MNP). The influence of pH on the reactivity is very small for both $\mathbf{1}_{0.4}$-MPGN-Zn(II) and reference **3**-Zn(II) in the interval 7−9.5 (SI, Figure S5), indicating that the catalytically relevant nucleophile, likely a metal bound hydroxide, is fully formed under these conditions.[6] The reactivity gain due to the confinement of the Zn(II) complexes on the nanoparticle monolayer is remarkable: at pH 7, $\mathbf{1}_{0.4}$-MPGN-Zn(II) hydrolyzes BNP 100 times faster than **3**-Zn(II) at the same concentration (50 μM) of the metal complex. The observed rate constant is 3.6×10^{-5} s^{-1} with a 300 000-fold acceleration over the background reaction.[7]

Figure 1a reports the reactivity of **1**-MPGN at pH 8.0 as a function of Zn(II) added. The reactivity levels off immediately after the addition of 1 equiv of Zn(II), indicating full binding of the metal ions to the **1** units.[8] The nonmonotonic increase of the reaction rate toward saturation suggests the presence of two different active species, depending on the Zn(II) loading of the nanoparticles. Plausibly, these two species can be identified as monometallic and dimetallic sites spontaneously formed at the nanoparticles surface, the first being predominant at low metal loadings, due to electrostatic repulsion, and the latter forming when a larger amount of metal complexes are formed.

Chart 1. Ligands and MPGN Schematic Structure (NP: *p*-Nitrophenyl)

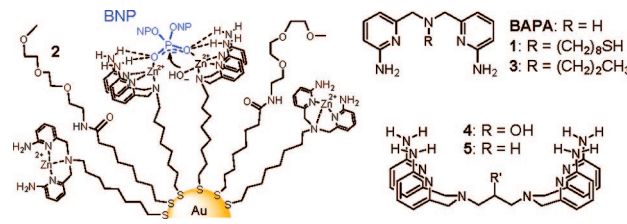

The kinetic profiles could be fitted with a model assuming the contribution of both of the species each with different reactivity and present in different amounts (see SI). The relevant parameters obtained are reported in Table 1 together with the affinity constants of the reactive species for phosphate diesters determined by competitive inhibition experiments with dimethyl phosphate (K_{DMP})[4,7] and, when possible, by Michaelis−Menten kinetics with BNP (K_{BMP}, see SI).[13] Analysis of the data summarized in Table 1 unveils several aspects of the reactivity of the MPGN. As can be expected (entries 5 and 7), the probability to form dimetallic sites on the particles at full metal loading depends on the relative concentration of ligand units in the monolayer. Thus, in the case of $\mathbf{1}_{0.4}$-MPGN 91% of **1** units can form dimetallic sites, while only a small fraction (30%) can do the same in the less concentrated monolayer of $\mathbf{1}_{0.1}$-MPGN. The reactivity of such dimetallic sites is 2 orders of magnitude larger than that of the monomeric reference complex **3**-Zn(II) (compare entries 2, 5, and 7). In systems where precom-

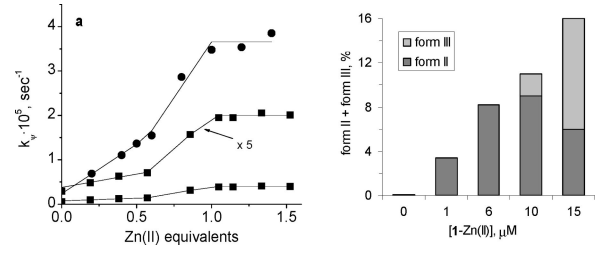

Figure 1. (a) Rates of BNP cleavage by $\mathbf{1}_{0.1}$-MPGN (■, [**1**] = 1.0×10^{-5} M) and $\mathbf{1}_{0.4}$-MPGN (●, [**1**] = 5.0×10^{-5} M) as a function of the equivalents of Zn(II) added at pH 8.0 (line: best fit of the data, SI). [HEPES] = 50 mM, [BNP] = 2×10^{-5} M, 40 °C; (b) Extent of pBR 322 plasmid DNA forms II and III produced after cleavage with different concentrations of $\mathbf{1}_{0.4}$-MPGN-Zn(II). [DNA_{bp}] = 12 μM. [HEPES] = 20 mM, pH 7, 37 °C, 24 h.

[†] Dipartimento di Scienze Chimiche, Università di Padova.
[‡] Dipartimento di Scienze Farmaceutiche, Università di Padova.
[§] Dipartimento di Chimica Fisica, Università di Venezia.

10.1021/ja801794t CCC: $40.75

Table 1. Apparent Second-Order Rate Constants (k_2) for BNP Cleavage, DMP Binding Constants (K_{DMP}), and Relative Reactivity (k_{rel}) for Different Zn(II)-Based Agents (pH 7, 40°C unless otherwise noted)

entry	catalyst	k_2 (s^{-1} M^{-1})	K_{DMP} (M^{-1})	k_{rel}	ref
1	OH^-	2.4×10^{-5} [a]	–	1	9
2	**3**-Zn(II)	0.012 [b]	1.0×10^2	500	*c*
3	**5**-$Zn(II)_2$	0.0055 [b]	3.1×10^2	230	*c*
4	$\mathbf{1_{0.1}}$-MPGN-Zn(II)	0.11 [b]	1.3×10^2	4583	*c*
5	[$\mathbf{1_{0.1}}$-MPGN-Zn(II)]$_2$	1.5 [b]	2.2×10^3 (4.7×10^4) [d]	62 500	*c*
6	$\mathbf{1_{0.4}}$-MPGN-Zn(II)	0.45 [b]	8.3×10^2	18 750	*c*
7	[$\mathbf{1_{0.4}}$-MPGN-Zn(II)]$_2$	1.4 [b]	3.7×10^3	58 333	*c*
8	pseudoHis-Zn(II)	0.0030 [e]	n. d.	125	10
9	BPAN-$Zn(II)_2$	1.7×10^{-4}	8.6×10^1 [d]	7	11
10	QX-TACN-$Zn(II)_2$	0.0042 [f]	n. d.	175	12

[a] 35 °C. [b] pH 8. [c] This work. [d] K_{BNP}. [e] 50 °C. [f] pH 11.

plexation of the substrate occurs, both binding and intrinsic reactivity of the catalytic site contribute to the second-order rate constant. K_{DMP} values reveal that in the present case most of the reactivity gain derives from enhanced binding.[14] Incidentally, such a high affinity for DMP further supports the dimetallic nature of these sites since the K_{DMP} values determined are much larger than those, lower than 100 M^{-1}, usually measured for monometallic Zn(II) complexes[4] and similar to that of 2.7×10^3 M^{-1} (pH 7, 25 °C) reported for the dimetallic complex **4**-$Zn(II)_2$.[4c] Moreover, in the case of $\mathbf{1_{0.1}}$-MPGN, for which the binding constants for both DMP and BNP could be obtained, a relevant hydrophobic contribution to binding is evident ($K_{BNP} = 20K_{DMP}$).

Remarkably, also the activity of the mononuclear sites on **1**-MPGN (entries 4 and 6) is considerably larger than that of reference **3**-Zn(II). In this case too, for both $\mathbf{1_{0.1}}$-MPGN and $\mathbf{1_{0.4}}$-MPGN nanoparticles, the data indicate a relevant contribution to the activity due to enhanced binding. The more pronounced effect observed with $\mathbf{1_{0.4}}$-MPGN could be the result of a combined interaction of the substrate with a monometallic complex and adjacent ammonium ions of protonated, uncomplexed ligands.

Comparison of the reactivity of **1**-MPGN with binuclear complex **5**-$Zn(II)_2$ (entry 3) gives full account of the effectiveness of the nanoparticles-based catalyst. In both cases two BAPA-Zn(II) units are held in proximity with a poorly preorganized arrangement, but while nanoparticles show high reactivity, **5**-$Zn(II)_2$ is even less efficient than the mononuclear counterpart **3**-Zn(II). Inspection of entries 8−10, summarizing the reactivity of the most efficient Zn-based catalysts for BNP so far reported, reveals that such behavior is not uncommon with binuclear Zn(II) complexes, which usually behave quite poorly with this substrate even in the case of preorganized systems.[1c] It is thus very remarkable that the spontaneous and flexible organization of the reactive sites on the **1**-MPGN monolayer forms binuclear Zn(II)-based catalytic sites with high activity.

The encouraging results obtained with BNP prompted us to exploit **1**-MPGN multivalency in the cleavage of a multivalent substrate like DNA. Considerable activity was indeed observed. Incubation of pBR 322 plasmid DNA with $\mathbf{1_{0.4}}$-MPGN-Zn(II) at pH 7.0 and 37 °C for 24 h resulted in its significant cleavage (Figure 1B), whereas no reaction at all was observed with monomeric **3**-Zn(II) (SI). The pseudo-first-order rate constant estimated at the maximum 15 μM Zn(II) complex concentration accessible[15] is 2×10^{-6} s^{-1}, a 5 orders of magnitude rate acceleration over uncatalyzed DNA hydrolysis.[16] Such a result appears even more remarkable if one considers that, for simple geometric reasons, only a fraction of the Zn(II) complexes present on a single nanoparticle can interact with the bound substrate. Most important, the amount of linear DNA (form III) formed is 50% larger than that of nicked DNA (form II). More than 100 single strand cleavage events are needed to obtain linearization in the case of a random process.[17] Thus, the formation of an amount of linear form largely exceeding the nicked one in the early stages of the reaction indicates that $\mathbf{1_{0.4}}$-MPGN-Zn(II) preferentially performs double strand cleavage.

The use of nanoparticles bearing an array of active units implies trading preorganization and rational design for flexibility and self-organization. The gain obtained on activity is impressive. The most effective Zn(II)-based catalyst so far reported provides a 36 000-fold acceleration for the cleavage of BNP at pH 7 and 3.6 mM complex concentration (Table 1, entry 8).[1c,10] $\mathbf{1_{0.4}}$-MPGN-Zn(II) at only 50 μM Zn(II) complex concentration produces a 300 000-fold rate acceleration (pH 7, 40 °C). The second-order rate constants measured for the dimetallic sites in the nanoparticles well compare with those observed for the most reactive lanthanide and Co(III) complexes.[7,9] The activity against DNA is less impressive but characterized by an unprecedented ability to perform double strand cleavage. Such behavior is typical of enzymes but extremely difficult to attain with artificial systems[1c] and can be ascribed to the multivalent nature of the nanoparticle-based catalyst. In fact, in the contact area between DNA and the nanoparticle surface, several reactive sites are present so that contemporaneous attack on both strands is possible.

Acknowledgment. Financial support by MUR (Contracts 2006034123 and 2006039071) is gratefully acknowledged.

Supporting Information Available: Synthesis; characterization of **1**, **5**, and **1**-MPGN; and kinetic experiments. This material is available free of charge via the Internet at http://pubs.acs.org.

References

(1) (a) Komiyama, M.; Takeda, N.; Shigekawa, H. *Chem. Commun.* **1999**, 1443–1451. (b) Niittymaki, T.; Lonnberg, H. *Org. Biomol. Chem.* **2006**, *4*, 15–25. (c) Mancin, F.; Tecilla, P. *New J. Chem.* **2007**, *31*, 800–817.
(2) (a) Pasquato, L.; Rancan, F.; Scrimin, P.; Mancin, F.; Frigeri, C. *Chem. Commun.* **2000**, 2253–2254. (b) Manea, F.; Houillon, F. B.; Pasquato, L.; Scrimin, P. *Angew. Chem., Int. Ed.* **2004**, *43*, 6165–6169. (c) Pengo, P.; Baltzer, L.; Pasquato, L.; Scrimin, P. *Angew. Chem., Int. Ed.* **2007**, *46*, 400–404. (d) Manea, F.; Bindoli, C.; Polizzi, S.; Lay, L.; Scrimin, P. *Langmuir* **2008**, *24*, 4120–4124.
(3) (a) Martin, M.; Manea, F.; Fiammengo, R.; Prins, L. J.; Pasquato, L.; Scrimin, P. *J. Am. Chem. Soc.* **2007**, *129*, 6982–6983. (b) Zaupa, G.; Prins, L. J.; Scrimin, P. *J. Am. Chem. Soc.* **2008**, *130*, 5699–5709.
(4) (a) Feng, G. Q.; Mareque-Rivas, J. C.; de Rosales, R. T. M.; Williams, N. H. *J. Am. Chem. Soc.* **2005**, *127*, 13470–13471. (b) Feng, G. Q.; Mareque-Rivas, J. C.; Williams, N. H. *Chem. Commun.* **2006**, 1845–1847. (c) Feng, G. Q.; Natale, D.; Prabaharan, R.; Mareque-Rivas, J. C.; Williams, N. H. *Angew. Chem., Int. Ed.* **2006**, *45*, 7056–7059.
(5) (a) Livieri, M.; Mancin, F.; Tonellato, U.; Chin, J. *Chem. Commun.* **2004**, 2862–2863. (b) Livieri, M.; Mancin, F.; Saielli, G.; Chin, J.; Tonellato, U. *Chem.—Eur. J.* **2007**, *13*, 2246–2256.
(6) pK_a of the Zn-bound water molecules in complex **3**-Zn(II) are 8.0 and 10.2 at 25 °C (ref 5). Lower values may be expected for $\mathbf{1_{0.4}}$-MPGN-Zn(II) due to electrostatic effects, as in metallomicelles; see: Bunton, C. A.; Scrimin, P.; Tecilla, P. *J. Chem. Soc., Perkin Trans. 2* **1996**, 419–213.
(7) The rate estimated for the spontaneous hydrolysis of BNP at pH 7.0 and 40 °C is 1.1×10^{-10} s^{-1}; see Chin, J.; Banaszczyk, M.; Jubian, V.; Zou, X. *J. Am. Chem. Soc.* **1989**, *111*, 186–190.
(8) Apparent Zn(II) binding constant for ligand **3** at pH 8 is $10^{6.5}$ at 25° C (data from ref 5), which ensures more than 90% complex formation.
(9) Yatsimirsky, A. K. *Coord. Chem. Rev.* **2005**, *249*, 1997–2011.
(10) Ichikawa, K.; Tarnai, M.; Uddin, M. K.; Nakata, K.; Sato, S. *J. Inorg. Biochem.* **2002**, *91*, 437–450.
(11) Kaminskaia, N. V.; He, C.; Lippard, S. J. *Inorg. Chem.* **2000**, *39*, 3365.
(12) Arca, M.; Bencini, A.; Berni, E.; Caltagirone, C.; Devillanova, F. A.; Isaia, F.; Garau, A.; Giorgi, C.; Lippolis, V.; Perra, A.; Tei, L.; Valtancoli, B. *Inorg. Chem.* **2003**, *42*, 6929–6939.
(13) Precipitation of the nanoparticles in the presence of an excess of the lipophilic BNP was observed with $\mathbf{1_{0.4}}$-MPGN.
(14) For cooperation in substrate binding and catalysis by functional units arranged on a surface see: (a) Major, R. C.; Zhu, X.-Y. *J. Am. Chem. Soc.* **2003**, *125*, 8454–8455. (b) Basabe-Desmonts, L.; Reinhoudt, D. N.; Crego-Calama, M. *Chem. Soc. Rev* **2007**, *36*, 993–1017; see also ref 3.
(15) DNA precipitation occurs when the overall concentration of metal complex exceeds that of the DNA (24 μM in residues).
(16) Uncatalyzed rate (pH 7.0 and 37 °C): 1×10^{-11} s^{-1}; see: Hettich, R.; Schneider, H.-J. *J. Am. Chem. Soc.* **1997**, *119*, 5638–5647.
(17) Branum, M. E.; Tipton, A. K.; Zhu, S.; Que, L., Jr. *J. Am. Chem. Soc.* **1996**, *123*, 1998–1904.

JA801794T